

STUDY ON SECOND HARMONIC GENERATION IN SiC USING INFRARED FEL

S. Tagiri[†], H. Zen, T. Kii, and H. Ohgaki,
 Institute of Advanced Energy, Kyoto University, Uji, Japan

Abstract

Mode-selective phonon excitation (MSPE) is an attractive method for studying the lattice dynamics (e.g. electron-phonon interaction and phonon-phonon interaction). In addition, MSPE can control electronic, magnetic, and structural phases of materials. In 2013, we have directly demonstrated MSPE of a bulk material (6H-SiC) with MIR-FEL (KU-FEL) by anti-Stokes (AS) Raman scattering spectroscopy. Recently, we have certified that the Sum Frequency Generation (SFG) also occurs with AS Raman scattering. For distinguishing between the AS Raman scattering and SFG, we need to know the nonlinear susceptibility and the transmittance. The coefficients can be measured by the Second Harmonic Generation (SHG) spectroscopy. This paper outlines of the measurement system and reports preliminary results with a 6H-SiC sample.

INTRODUCTION

The electron-phonon interaction influences physical properties of solid-state materials. Thus, the clarification of the interaction is required for understanding basic physical properties of solid-state materials and developing high-performance devices [1,2]. To clarify the interaction, it is important to understand the relation between the electronic state and the excitation of a particular lattice vibration (phonon). Mode-selective phonon excitation (MSPE) is one of the attractive methods in the solid-state physics because it can be a powerful tool for the study of ultrafast lattice dynamics (e.g. electron-phonon interaction and phonon-phonon interaction). Not only for that, but MSPE can control electronic, magnetic, and structural phases of ma-

terials [3-5]. By irradiating a mid-infrared pulse laser tuned to the resonant wavelength of a specific phonon, the direct excitation of a specific phonon mode is available [3,5].

We have developed a technique which can directly observe the vibration of a particular phonon mode by using AS Raman scattering spectroscopy (Fig. 1) [6]. By using the technique, the MSPE induced by MIR-FEL has been directly demonstrated with a bulk material of 6H-SiC (Fig. 2)[7]. However, we have certified that SFG also occurs together with AS Raman scattering. For distinguishing between the AS Raman scattering and SFG, we need to know the nonlinear susceptibility and the transmittance. In the previous study at FHI-FEL [8], the wavelength dependence of nonlinear susceptibilities $\tilde{\chi}^{(2)}$ of 4H-SiC and 3C-SiC in MIR region have been experimentally characterized by the SHG spectroscopy.

The SHG intensity scales linearly with nonlinear polarization P , which can be given by the formula [9],

$$\vec{P}(2\omega) = \tilde{\chi}^{(2)}(2\omega, \omega, \omega) : \left(\vec{L}_1(\omega) \vec{E}_1(\omega) \right) \left(\vec{L}_2(\omega) \vec{E}_2(\omega) \right),$$

where ω denotes frequency of incident light. The frequency of SHG is twice as great as it of incident light. $\vec{L}_{1(2)}$ are the Fresnel transmission tensors for two incident beams representing the macroscopic local field corrections [10], and $\vec{E}_{1(2)}$ are the incident electric field vectors. The Fresnel transmission tensor can be evaluated by theoretical calculation. The nonlinear susceptibility must be experimentally determined by the equation of SHG spectroscopy in the reference [8]. The reflected second harmonic intensity is given by projecting the nonlinear polarization onto the field direction of the reflected [10].

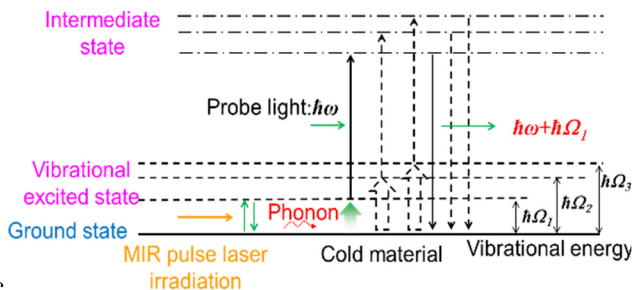


Figure 1: Schematic of the principle of demonstration experiment of MSPE induced by MIR-FEL irradiation. The anti-Stokes-Raman scattering was utilized to observe the excited state [3].

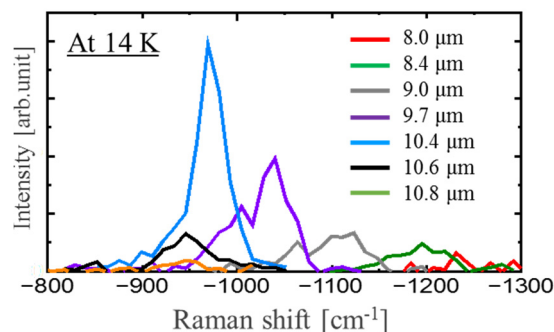


Figure 2: Anti-Stokes Raman scattering spectra measured with MIR-FEL and pico-second laser at 14K [7].

[†] tagiri.shunsuke.53a@st.kyoto-u.ac.jp

Content from this work may be used under the terms of the CC BY 3.0 licence (© 2018). Any distribution of this work must maintain attribution to the author(s), title of the work, publisher, and DOI.

In this study, a SHG spectroscopy system has been developed at a MIR-FEL facility, KU-FEL, for determining the nonlinear susceptibility of 6H-SiC. The preliminary experimental results are reported in this paper.

CALCULATION

We calculate Fresnel transmission coefficient $L_{xx(yy)zz}$ of 6H-SiC based on the equations in the previous report [8]. The equations are as follows:

$$L_{xx}(\omega, \theta^i) = \frac{2k_{z,e}^{SiC}(\omega, \theta^i)}{\epsilon_{\perp}(\omega)k_z^{air}(\omega, \theta^i) + k_{z,e}^{SiC}(\omega, \theta^i)} \quad (1)$$

$$L_{yy}(\omega, \theta^i) = \frac{2k_z^{air}(\omega, \theta^i)}{k_z^{air}(\omega, \theta^i) + k_{z,o}^{SiC}(\omega, \theta^i)} \quad (2)$$

$$L_{zz}(\omega, \theta^i) = \frac{\epsilon_{\perp}(\omega)}{\epsilon_{\parallel}(\omega)} \frac{2k_z^{air}(\omega, \theta^i)}{\epsilon_{\perp}(\omega)k_z^{air}(\omega, \theta^i) + k_{z,e}^{SiC}(\omega, \theta^i)} \quad (3)$$

$$\epsilon_{\perp}(\omega) = \epsilon_{\perp}^{\infty} \left(1 + \frac{\omega_{LO,\perp}^2 - \omega_{TO,\perp}^2}{\omega_{TO,\perp}^2 - \omega^2 - i\omega\gamma_{TO,\perp}} \right) \quad (4)$$

$$\epsilon_{\parallel}(\omega) = \epsilon_{\parallel}^{\infty} \left(1 + \sum_{j=0,1} \frac{\omega_{LO,\parallel j}^2 - \omega_{TO,\parallel j}^2}{\omega_{TO,\parallel j}^2 - \omega^2 - i\omega\gamma_{TO,\parallel j}} \right) \quad (5)$$

$$k_{z,o}^{SiC}(\omega, \theta^i) = \frac{2\pi\omega}{c_0} \sqrt{\epsilon_{\perp}(\omega) - \sin^2(\theta^i)} \quad (6)$$

$$k_{z,e}^{SiC}(\omega, \theta^i) = \frac{2\pi\omega}{c_0} \sqrt{\epsilon_{\perp}(\omega) - \frac{\epsilon_{\perp}(\omega)}{\epsilon_{\parallel}(\omega)} \sin^2(\theta^i)} \quad (7)$$

The parameters used to calculate the Fresnel transmission coefficient are listed in Table 1.

Result of calculation of the Fresnel transmission coefficients are shown in Fig. 3. L_{xx} and L_{yy} have a peak at 970–980 cm^{-1} . On the other hand, L_{zz} has a peak at 1055 cm^{-1} . In this wavenumber region, the nonlinear susceptibility of 6H-SiC is not expected to have any peak similar to 3C-SiC and 4H-SiC [8]. Therefore, it is expected that the observed peaks of SHG at 975 cm^{-1} and 1055 cm^{-1} are due to the high Fresnel transmission coefficient.

Table 1: Parameters Used to Calculate the Fresnel Transmission Coefficient of 6H-SiC [8,11-14]

	ω_{TO}	ω_{TO}	ω_{TO}	ϵ_{∞}
Planar strong	797 cm^{-1}	3.5 cm^{-1}	969.9 cm^{-1}	6.58
Axial strong	788 cm^{-1}	3.5 cm^{-1}	965 cm^{-1}	6.72
Axial weak	775 cm^{-1}	1.85 cm^{-1}	889 cm^{-1}	-

EXPERIMENT CONDITIONS AND SETUP

We used a 6H-SiC sample which is the same sample used in the previous studies [6, 7, 15]. It was a commercially available semi-insulator type 6H-SiC (Xlamen Powerway Advanced Material Co., LTD) with dimension of 15 mm × 15 mm × 0.33 mm and the crystal orientation of (0001). The known phonon modes of 6H-SiC around 10 μm are listed in Table 2 [11].

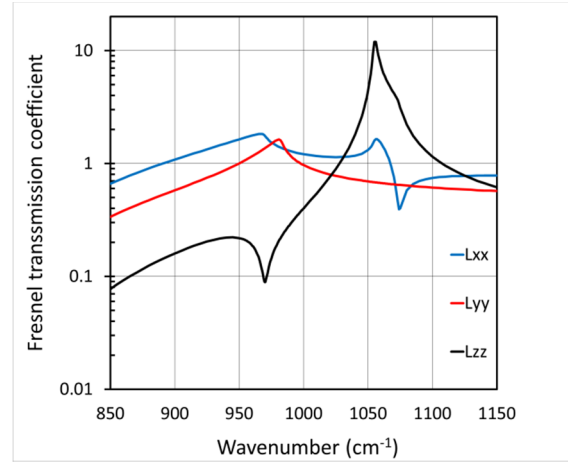


Figure 3: Calculated Fresnel transmission coefficient of 6H-SiC by the reference experiment [7].

Table 2: Phonon Modes of 6H-SiC [11]

wavenumber (wavelength)	infrared	Raman
965 cm^{-1} (10.4 μm)	active	active
797 cm^{-1} (12.5 μm)	active	inactive
787 cm^{-1} (12.7 μm)	inactive	active
767 cm^{-1} (13.0 μm)	inactive	active

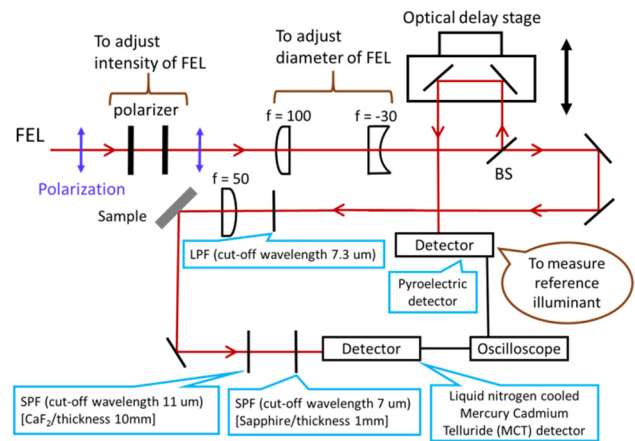


Figure 4: Schematic of the experimental setup.

Content from this work may be used under the terms of the CC BY 3.0 licence (© 2018). Any distribution of this work must maintain attribution to the author(s), title of the work, publisher, and DOI.

The schematic of the experimental setup is illustrated in Fig. 4. To adjust the intensity of FEL irradiated on the 6H-SiC sample, two wire-grid polarizers were used. In order to keep the polarization angle of FEL beam on the sample, the angle of second polarizer was kept constant and that of first polarizer was varied for changing the total attenuation of this polarizer pair. A telescope was used to reduce the beam size by one third.

We split FEL beam into two with a beam splitter and simultaneously measured the SHG and incident FEL intensities. SHG was measured by a highly sensitive liquid nitrogen cooled MCT detector (J15D12, Judson). A long pass filter was used to block the harmonic components inherently included in FEL. The FEL beam was focused on the sample using a focusing lens. The fundamental beam was blocked by a 10-mm thick CaF₂ plate and a 1-mm thick sapphire plate so as to inject only SHG beam on to the MCT detector. The polarization of incident light was adjusted to P-polarization, because P-polarization was used in the previous MSPE experiments [6,7,15].

At first, we confirmed the relationship between the intensity of irradiated pulse and MCT signal with changing FEL intensity. Next, relative SHG efficiencies as the function of the incident FEL wavelength were measured.

RESULTS AND DISCUSSION

The measured relationship between the intensity of incident FEL pulse and the signal intensity measured by the MCT detector at the wavelength of 8.0 μm is shown in Fig. 5. The fitting curve whose function is $y = ax^2 + b$ (red line) is also plotted in Fig. 5. The observed MCT signal intensity follows a quadratic dependence on the intensity of the incident FEL. As the result, it was confirmed that the measured signal is SHG generated on the 6H-SiC sample.

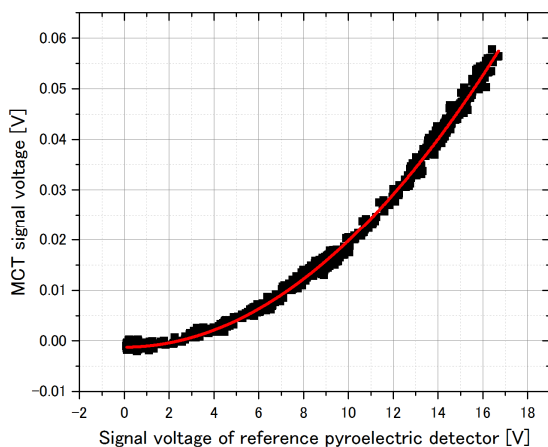


Figure 5: Relationship between the intensity of FEL pulse and the signal intensity measured by the MCT detector. Black dots represent the measured data. Red line represents the fitting curve with the function of $y = ax^2 + b$.

Next, the second-order coefficients of FEL intensity dependences at each FEL wavelength were measured to determine the SHG efficiency dependence on the wavelength. We adjusted the angle of the mirror arranged after the sample by fundamental beam without the CaF₂ and sapphire plates. The result of the second-order coefficient dependence on the FEL wavelength is shown in Fig. 6. In this case, single weak peak was observed at 970 cm⁻¹ while the highest second-order coefficient was observed at 1111 cm⁻¹.

After that, we adjusted the mirror after the sample to have the highest SHG signal on the MCT detector at each FEL wavelength. The measured dependence of the second-order coefficient on the FEL wavenumber is shown in Fig. 7. In this case, two peaks around 970 cm⁻¹ and 1050 cm⁻¹ were observed. This result suggested that the angular distribution of SHG has strong wavelength dependence, because we needed to adjust the mirror angle to obtain the maximum intensity for each wavelength. Under the assumption that $\chi^{(2)}$ possesses no peak in this wavenumber region as reported [9], a small peak expected to appear around 970 cm⁻¹, and a large peak expected to appear around 1055 cm⁻¹ from the calculated result of the Fresnel transmission coefficient shown in Fig. 3. Figure 7 indicates two peaks in these corresponding wavenumbers.

As a result, we successfully observed SHG signal from 6H-SiC. We could deduce that the angular distribution of the SHG depends on the FEL wavelength from the comparison of the second-order coefficients shown in Figs. 6 and 7. The measured SHG dependence on the FEL wavelength was not sharp as 4H-SiC and 3C-SiC as reported [8]. Further investigation of the developed measurement system need to be performed.

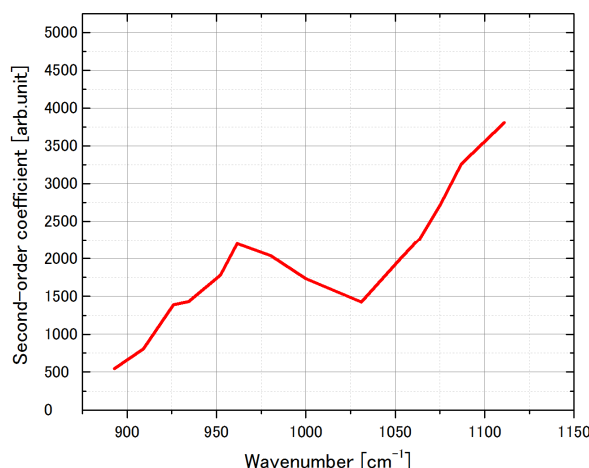


Figure 6: The second-order coefficient when we adjusted optical axis by fundamental wave and fixed optical axis.

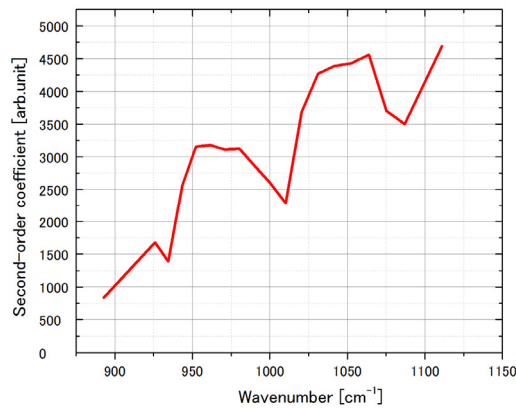


Figure 7: The second-order coefficient when we adjusted the angle of a mirror after the sample at each wavelength to get maximum SHG signals.

CONCLUSION

A SHG spectroscopy system has been developed to measure the second-order nonlinear susceptibility of 6H-SiC in the MIR region. It was confirmed that the SHG generated on the 6H-SiC sample can be measured by the developed system. The wavelength dependence of SHG intensity had some similarity with the calculated Fresnel transmission. The spatial distribution of the SHG depends on the wavelength.

REFERENCES

- [1] K. Kato *et al.*, *J. Appl. Phys.* 111, 113520 (2012).
- [2] T. Sonobe *et al.*, *AIP Conf. Proc.* 1214, 23 (2010).
- [3] M. Rini *et al.*, *Nature* 449, 72-74 (2007).
- [4] M. Först *et al.*, *Phys. Rev. B* 84, 241104 (2011).
- [5] D. Fausti *et al.*, *Science* 331, 189 (2011).
- [6] K. Yoshida *et al.*, *Appl. Phys. Lett.* 103, 182103 (2013).
- [7] T. Murata, thesis for Masters degree, Kyoto University, (2016).
- [8] A. Paarmann *et al.*, *Phys. Rev. B* 94, 134312 (2016).
- [9] A. Paarmann *et al.*, *Appl. Phys. Lett.* 107, 081101 (2015).
- [10] Y.R. Shen, *Annu. Rev. Phys. Chem.* 40, 327 (1989).
- [11] S. Nakashima and H. Harima, *Phys. Stat. Sol. A* 162, 39 (1997).
- [12] H. Mutschke, A. Andersen, D. Clement, T. Henning, and G. Peiter, *Astron. Astrophys.* 345, 187 (1999).
- [13] F. Engelbrecht and R. Helbig, *Phys. Rev. B* 48, 15698 (1993).
- [14] J. Bluet, K. Chourou, M. Anikin, and R. Madar, *Materials Science and Engineering B* 61-62, 212 (1999).
- [15] T. Katsurayama *et al.*, *Proc. of IRMMW-THz'16*, T5P.25.05.